

Interaction of tau protein with the dynactin complex

Enrico Magnani^{1,4}, Juan Fan^{2,4},
Laura Gasparini¹, Matthew Golding³,
Meredith Williams¹, Giampietro Schiavo³,
Michel Goedert², Linda A Amos²
and Maria Grazia Spillantini^{1,*}

¹Department of Clinical Neurosciences, Brain Repair Centre, University of Cambridge, Cambridge, UK, ²Medical Research Council Laboratory of Molecular Biology, Cambridge, UK and ³Cancer Research UK London Research Institute, London, UK

Tau is an axonal microtubule-associated protein involved in microtubule assembly and stabilization. Mutations in *Tau* cause frontotemporal dementia and parkinsonism linked to chromosome 17 (FTDP-17), and tau aggregates are present in Alzheimer's disease and other tauopathies. The mechanisms leading from tau dysfunction to neurodegeneration are still debated. The dynein-activator complex dynactin has an essential role in axonal transport and mutations in its gene are associated with lower motor neuron disease. We show here for the first time that the N-terminal projection domain of tau binds to the C-terminus of the p150 subunit of the dynactin complex. Tau and dynactin show extensive colocalization, and the attachment of the dynactin complex to microtubules is enhanced by tau. Mutations of a conserved arginine residue in the N-terminus of tau, found in patients with FTDP-17, affect its binding to dynactin, which is abnormally distributed in the retinal ganglion cell axons of transgenic mice expressing human tau with a mutation in the microtubule-binding domain. These findings, which suggest a direct involvement of tau in axonal transport, have implications for understanding the pathogenesis of tauopathies.

The EMBO Journal (2007) 26, 4546–4554. doi:10.1038/sj.emboj.7601878; Published online 11 October 2007

Subject Categories: cell & tissue architecture; neuroscience
Keywords: axonal transport; dynactin; microtubule-binding; tau; tauopathies

Introduction

The neuronal microtubule (MT)-associated protein tau plays an important role in the organization of axonal MTs (Lee *et al*, 2001). Tau is also the major component of the neurofibrillary pathology that defines Alzheimer's disease and other related neurodegenerative disorders. Furthermore, mutations

in the tau gene cause a familial form of dementia (fronto-temporal dementia and parkinsonism linked to chromosome 17 (FTDP-17)), indicating that dysfunction of tau protein is sufficient to cause neurodegeneration (Yancopoulos and Spillantini, 2003). In adult human brain, there are six tau isoforms produced from a single gene by alternative mRNA splicing (Goedert *et al*, 1989). They differ by the presence of three or four MT-binding repeats in the C-terminal region (with the extra repeat encoded by exon 10) and the presence or absence of 29 or 58 amino-acid inserts (encoded by exons 2 and 3) in the N-terminal region. Tau consists of two major parts, a C-terminal MT-binding region and an N-terminal projection domain (Hirokawa *et al*, 1988; Kar *et al*, 2003a). Unlike the MT-binding region, relatively little is known about the function of the projection domain. It has previously been implicated in determining the spacing between MTs (Chen *et al*, 1992) and in mediating the interactions between tau and the plasma membrane (Brandt *et al*, 1995). Interestingly, mutations of a conserved arginine (R5) in exon 1 have been implicated in cases of human dementia (Hayashi *et al*, 2002) and progressive supranuclear palsy (Poorkaj *et al*, 2002).

The dynactin complex is found in many cell types, including neurons, and plays an important role in mediating the binding of the MT motor complex dynein to its membranous cargoes (Holzbaur *et al*, 1991; Schroer, 2004). Dynactin consists of a short filament of an actin-like protein, ARP1, and around 10 other polypeptides, including a dimer of the heavy chain, known as p150. This extended protein binds alongside the ARP1 filament and forms a sideways coiled-coil extension, tipped with a pair of globular N-terminal domains. The latter are MT-binding CAP-Gly domains (Schroer, 2004). The ARP1 filament is thought to be able to interact with the layers of actin filaments that lie in contact with cell membranes. Dynactin plays an essential role in axonal transport (Holzbaur *et al*, 1991; Waterman-Storer *et al*, 1997; Schroer, 2004) and its mutations have been associated with motor neuron disease (Puls *et al*, 2003, 2005; Münch *et al*, 2005).

Here we show that the projection domain of tau interacts directly with the C-terminus of p150 the major component of the dynein-activator complex dynactin. This binding is affected by the mutation of a conserved arginine residue in position 5 in exon 1 of the tau gene, which causes FTDP-17 (Hayashi *et al*, 2002; Poorkaj *et al*, 2002). We also show that tau facilitates the binding of p150 to MTs and that tau and p150 are colocalized and abnormally distributed in retinal ganglion cell (RGC) axons from a transgenic mouse line expressing human tau with the P301S mutation in the MT-binding domain (Allen *et al*, 2002).

Results

Bacterial two-hybrid screen

A bacterial two-hybrid screen of a human brain cDNA library using exons 1–4 of *Tau* (Figure 1) as the bait yielded five positives, one of which corresponded to the 113 C-terminal

*Corresponding author. Department of Clinical Neurosciences, Brain Repair Centre, University of Cambridge, Robinson way, Forvie site, Cambridge CB2 0PY, UK. Tel.: +44 1223 331145;

Fax: +44 1223 331174; E-mail: mgs11@cam.ac.uk

⁴These authors contributed equally to this work

Received: 18 December 2006; accepted: 12 September 2007;
published online: 11 October 2007

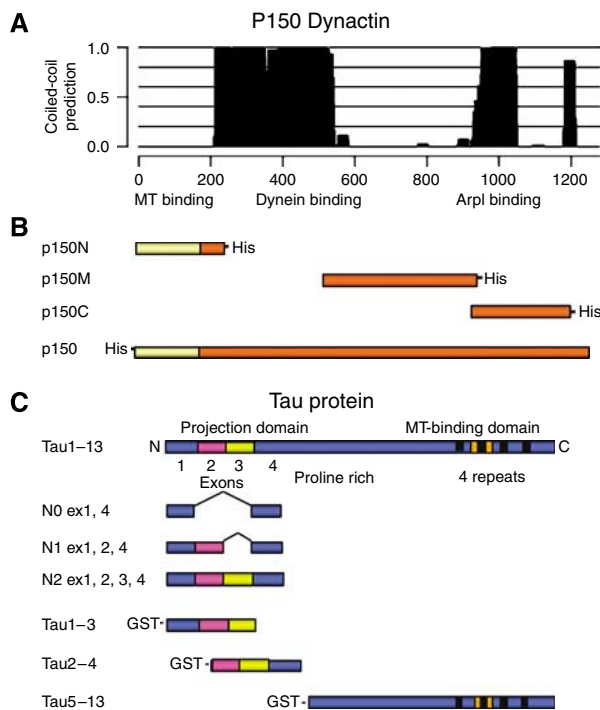


Figure 1 Schematic representation of dynactin p150 functional domains and dynactin p150 and tau DNA fragments used for *in vitro* experiments. (A) p150 functional domains and associated coiled-coil domains (plot); dynein- and ARP1-binding domains overlap with two main coiled-coil domains in the protein structure; a small coiled-coil domain is present near the C-terminus, around aa 1200, overlapping with the tau-interacting region identified in this work. (B) His-tagged N-terminal (p150N; aa 1–210), central (p150M; aa 550–940), C-terminal (p150C; aa 900–1200) and full-length p150 used for *in vitro* binding experiments. (C) The 441-amino-acid isoform of human brain tau (htau40, exons 1–13) contains a C-terminal MT-binding domain with 4 repeats (black boxes) one of which (encoded by exon 10, indicated in orange) is missing from tau isoforms with three repeats. The N-terminus contains alternatively spliced exon 2 (magenta) and exon 3 (yellow). Full-length tau1–13 and fragments N0, N1 and N2 were used in the bacterial two-hybrid screening. Tau1–13 and GST-tagged tau1–3, tau2–4 and tau5–13 constructs were used for *in vitro* binding experiments.

amino acids of p150 (residues 1166–1278). The latter was then used as the bait against full-length tau or against constructs consisting of *Tau* exons 1 and 4; exons 1, 2 and 4; and exons 1–4. Full-length tau1–13 (the 441-amino-acid isoform of human brain tau (clone htau40)) and all three N-terminal fragments interacted with the C-terminal part of p150. These results indicated that the interaction occurs between the C-terminus of dynactin and the sequence encoded by exons 1 and 4 at the N-terminus of tau, whereas exons 2 and 3 are not necessary for this binding.

***In vitro* binding assays of tau and dynactin**

To further characterize the association between tau and p150, we performed *in vitro* binding assays of a range of recombinant protein fragments. GST-tagged tau fragments and His-tagged p150 fragments were bound to magnetic beads coated with anti-tag antibodies and interacting proteins were visualized by SDS-PAGE and immunoblotting (Figure 2). Besides wild-type tau, R5H and R5L tau mutants as well as partial sequences consisting of exons 1–3, 2–4 and 5–13 (tau1–3,

tau2–4 and tau5–13, respectively) were used (Figure 1). Full-length p150 (which tended to aggregate and degrade into shorter fragments, even after isolation), an N-terminal fragment (residues 1–210, p150N), a middle fragment (residues 550–940, p150M) and a near C-terminal fragment (residues 900–1200, p150C) were tested (Figure 1). Several alternative C-terminal fragments containing the sequence after residue 1200 were expressed as insoluble protein and could not be used.

Full-length p150 as well as the p150C fragment bound to GST-tagged tau1–3 or tau2–4, which also interacted with a detectable amount of native dynactin complex (Figure 2A–C and E). Fragments p150N and p150M, however, did not bind to tau fragments containing the projection domain (Figure 2A–C). These findings indicate that the tau-binding site lies within the C-terminal 338 amino acids of p150. However, neither p150C nor full-length p150 bound to the tau5–13 GST fusion protein (Figure 2A, D and E). When full-length His-tagged p150 or p150C was used as bait, full-length tau1–13 and its N-terminal fragments did bind (Figure 2F–H), whereas tau5–13 did not (Figure 2F). In contrast, when p150N or p150M was used as bait, no tau proteins bound (Figure 2G and H). These findings, summarized in Figure 2A, confirm that the p150-binding site lies on an extended part of the projection domain of tau, encoded by exons 1–4.

Effect of tau N-terminal mutations R5L and R5H

Since mutations R5L and R5H are known to cause tau dysfunction and aggregation *in vivo*, we expressed full-length tau proteins containing these mutations and investigated their interaction with p150C in pull-down assays. As shown in Figure 3, p150-associated magnetic beads are able to pull down a clearly detectable amount of wild-type tau. However, only a trace amount of tauR5L and no tauR5H bound to the beads. Thus, when tau's exon 1 sequence is present, residue R5 is very important for the binding to dynactin.

Binding of dynactin complex to MTs with and without tau

Tau and p150 have distinct MT-binding domains (Waterman-Storer *et al*, 1995; Lee *et al*, 2001). In order to clarify whether their interaction modulates their individual MT-binding properties, and to gain insight into the physiological role of this interaction, we investigated the binding of dynactin to MTs *in vitro* in the presence and absence of tau. MTs were assembled from purified pig brain tubulin with and without recombinant full-length tau, incubated either with whole dynactin complex purified from pig brain or with recombinant p150, and then pelleted. Dynactin fragments p150M and p150C did not bind to MTs under any condition. Tau and p150N were found to compete for binding sites on the MT surface. The presence of tau did not significantly change the amount of p150N in the pellet, but less tau appeared in the pellet when p150N was present than when it was absent (data not shown). It is not surprising that p150N is able to displace some tau, since excess tau molecules bind to the outer surface of an MT by means of multiple weak binding sites (Kar *et al*, 2003b; Makrides *et al*, 2004). Whole native dynactin complex purified from pig brain (see Materials and methods) also bound to MTs and pelleted with them, irrespective of tau's presence or absence. However, the amount of dynactin complex in the pellet increased when tau was included (Figure 4A and B).

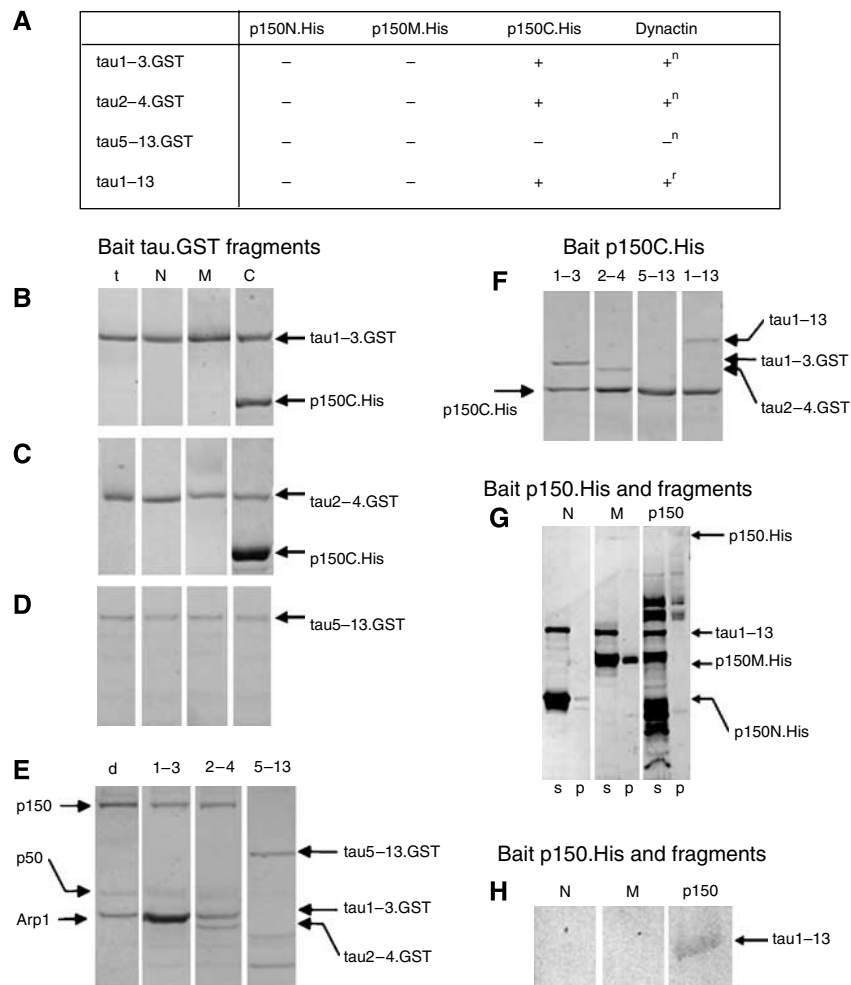


Figure 2 Binding of tau, dynactin p150 and their fragments. (A) Table summarizing the results of *in vitro* binding of tau.GST and p150.His or native dynactin complex using anti-tag-coated magnetic beads. (-), no binding; (+), binding observed. (n) native dynactin and (r) recombinant dynactin p150 were used in these experiments. (B-G) SDS-PAGE analysis of protein complexes interacting with anti-GST and anti-His antibodies on beads. Gels show proteins eluted from the beads and stained with Page-Blue 83. All the results were confirmed by immunoblotting (not shown). (B-D) GST-tagged recombinant tau fragments (B, tau1-3.GST; C, tau 2-4.GST; D, tau 5-13.GST) were used as bait for interaction with p150 and its fragments. t, only tau.GST fragments mixed with beads; N: tau.GST fragments with p150N.His; M: tau.GST fragments with p150M.His; C: tau.GST fragments with p150C.His. Only p150C.His binds to tau1-3 and 2-4 GST-tagged fragments. (E) Tau.GST fragments were used as bait for the native dynactin complex. d, native dynactin complex alone. d, native dynactin complex alone (p150, p50 and ARP1 are visible); 1-3: tau1-3.GST with native dynactin; 2-4: tau 2-4.GST with native dynactin; 5-13: tau 5-13.GST with native dynactin. Tau1-3.GST and tau 2-4.GST bind to native dynactin, but the tau 5-13.GST fragment does not. (F) p150C.His was used as bait and its interaction with tau.GST fragments and untagged full-length tau1-13 was tested. 1-3: p150C.His with tau1-3.GST; 2-4: p150C.His with tau2-4.GST; 5-13: p150C.His with tau5-13.GST; 1-13: p150C.His with full-length tau1-13.GST. tau1-3.GST, tau2-4.GST and tau1-13.GST bind to p150C.His but not the tau5-13.GST fragment. (G) SDS-PAGE of protein complexes interacting with p150.His constructs bound to anti-His antibodies on beads. Interaction of full-length tau1-13 with p150N.His (lane 1), p150M.His (lane 2) and recombinant full-length p150.His and fragments (lane 3). Since full-length His-tagged p150 had a strong tendency to aggregate and degrades during purification, only a small amount was available for binding to beads. Therefore, the untagged full-length tau protein that bound to p150.His on the beads was detected by immunoblotting with the anti-tau antibody BR133 as shown in (H). (H) Immunoblot of pellets in lanes 1-3 of panel G using BR133 of proteins interacting with p150N.His, p150M.His and p150.His bound to anti-His antibodies on beads. N: untagged full-length tau1-13 with p150N.His; M: untagged full-length tau1-13 with p150M.His; p150: untagged full-length tau1-13 with full-length p150.His. Tau1-13 binds to full-length recombinant dynactin (p150.His) but not to its fragments p150M.His and p150N.His.

The association between MTs and the native dynactin complex was investigated further by negative stain electron microscopy. When pig brain dynactin complex was added to the sample, we saw structures resembling the dynactin complex described by Schafer *et al* (1994), which were not visible when only tau was present. Complex-like structures attached to the MT appeared similar in the absence of tau or presence of N-terminally mutated tau, but were always rather sparse. In a typical experiment, we counted an average of 22 ± 4 ($n = 3$) projections per micrometer of MT when full-length wild-type tau was present, compared with an average of 8 ± 2

($n = 3$) when either no tau or R5L-tau was present. In order to identify these MT-interacting structures, we carried out immunolabelling with an anti-p150 primary antibody followed by gold-conjugated secondary label and found that gold particles decorated the entire lengths of MTs assembled in the presence of normal tau (Figure 5A). When dynactin complex was added to MTs assembled with N-terminally mutated tau, however, the amount of label along the MT was similar to background level (Figure 5B). The difference in decoration seen by EM is greater than that measured in the pelleting assay (Figure 4), possibly because any aggregated

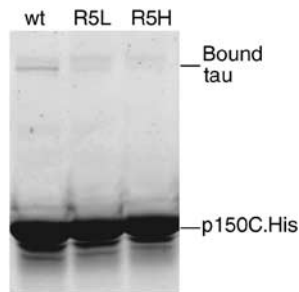


Figure 3 Pull-down assays of mutant tau and the C-terminal fragment of p150. SDS-PAGE of proteins bound to magnetic beads coated with anti-His antibodies. Dynactin fragment p150C.His was incubated with wild-type tau1-13 (lane 1), tauR5L (lane 2) and tauR5H (lane 3). Wild-type tau1-13 binds to p150C, but mutant tau1-13 R5L and R5H show a much reduced and absent binding, respectively.

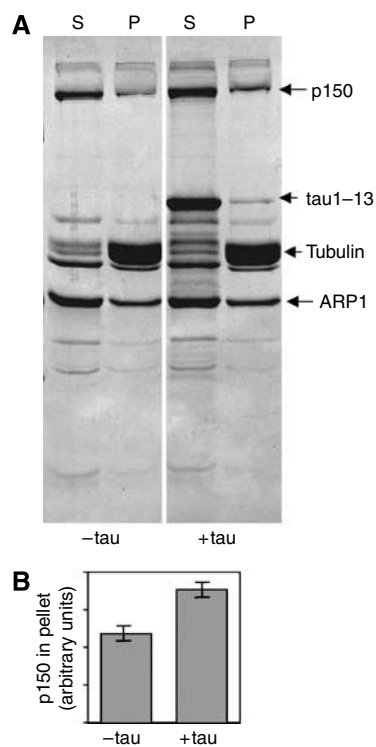


Figure 4 *In vitro* interaction of native dynactin complex with MTs and the effect of tau. (A) SDS-PAGE of proteins in the pellet (P) and supernatant (S), when purified native pig brain dynactin was incubated with MT assembled from purified pig brain tubulin, with or without recombinant tau1-13. (B) Integrated densities (in arbitrary units) obtained by densitometry of p150 bands in the pellet lanes of panel A.

group of molecules was counted as a single projection and the dynactin appeared to aggregate less when wild-type tau was present. When tau was not present, dynactin appeared to aggregate particularly at the ends of MTs.

In higher magnification images, the actin-like filaments that form part of the complex can be seen extending sideways from the ends of fine projections from the MT outer surface (Figure 5C–E). When tau was present, we often saw such structures in series, at intervals of ~30 or 40 nm (Figure 5A and C). There is a potential binding site for a dynactin projection on every tubulin heterodimer in the MT lattice,

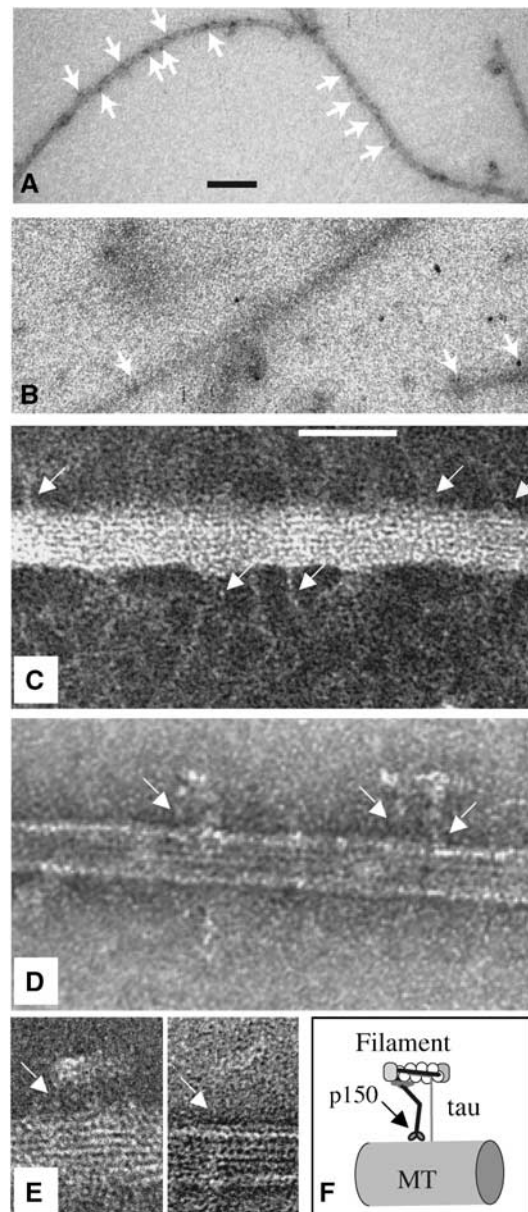


Figure 5 Electron microscopy and immunoelectron microscopy of native dynactin complex on MTs. (A, B) Immunoelectron microscopy of native dynactin bound to MT and labeled with anti-p150 and protein A conjugated with 20 nm gold and then negatively stained. Arrows point to gold particles on MT. MT in panel A were assembled with 4 μ M full-length wild-type tau, those in panel B with 4 μ M R5L mutant tau. Scale bar, 100 nm. (C–E) Negative staining images of MT assembled with 4 μ M wild-type tau and decorated with native dynactin. Arrows indicate fine dynactin-like stalks, tethering short ARP1 filaments to the MT. Scale bar, 50 nm. (F) A model of the way that p150 in the dynactin complex interacts with an MT and the projection domain of tau, as indicated by data in Figures 2–5.

8 nm apart along each protofilament, but either the actin-like filaments prevent the complexes from binding so closely and/or the intervals may be determined by the space between tau projections.

Localization and immunoprecipitation of tau and dynactin in differentiated SH-SY5Y cells

To look for an interaction between p150 and tau in living cells, we used untransfected, differentiated human neuro-

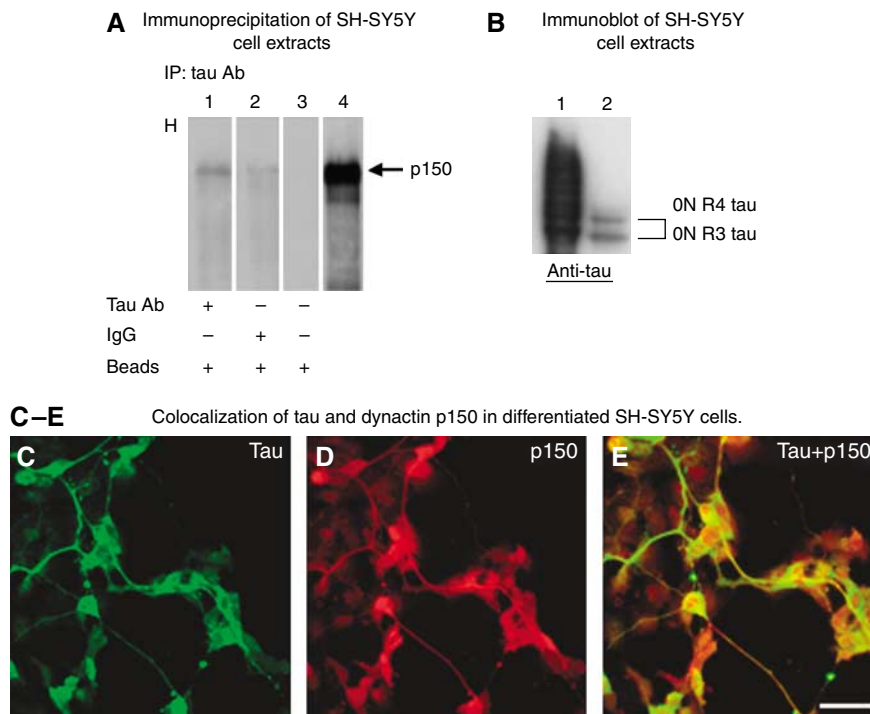


Figure 6 Localization and immunoprecipitation of tau and dynactin in differentiated SH-SY5Y cells. **(A)** Endogenous p150 co-immunoprecipitates with tau in differentiated SH-SY5Y cells. Immunoprecipitation was performed with anti-tau antibody BR133 and immunoblots with p150 antibody. p150 dynactin is present in the pellet containing immunoprecipitated proteins (lane 1). Normal rabbit IgG instead of BR133 (lane 2), only beads (lane 3) and whole-cell extract (lane 4) were used as controls. **(B)** SH-SY5Y cells express only the shortest three- and four-repeat tau isoforms as detected by immunoblotting of cell extracts with anti-tau antibody BR133. Lane 1, six recombinant human tau isoforms; lane 2, SH-SY5Y extracts. The two shortest tau isoforms with three and four repeats and no N-terminal inserts are present. **(C-E)** Tau and p150 colocalized in the cellular compartments of differentiated SH-SY5Y cells. Immunofluorescence labelling of tau **(C)** obtained with anti-tau antibody BR133, p150 **(D)** stained using anti-p150 antibody and overlay **(E)**. Scale bar: 40 μ m for panels C, D, E.

blastoma SH-SY5Y cells, which express tau and p150. In our experimental conditions (10 μ M retinoic acid (RA) for 2 weeks, 50 ng/ml brain-derived neurotrophic factor (BDNF) for 4 days), SH-SY5Y cells express only the shortest three- and four-repeat tau isoforms without amino terminal inserts (Figure 6B). By immunoprecipitation with anti-tau antibody BR133, a fraction of p150 co-sedimented with these tau isoforms (Figure 6A and B), consistent with the finding from the bacterial two-hybrid experiments that exons 2 and 3 of tau are not required for p150 binding. Not all dynactin p150 is immunoprecipitated by anti-tau antibodies, as expected by the higher abundance of dynactin p150 in SH-SY5Y cell extracts. Immunoprecipitation using anti-p150 antibodies was also performed, but tau runs at the same level as the antibody chains and the nonspecific background did not produce results clear enough to be shown. Immunocytochemistry shows that tau and dynactin p150 co-localize in the cellular compartments of differentiated SH-SY5Y cells (Figure 6C-E).

Localization of tau and p150 dynactin in RGC axons of transgenic mice expressing mutant P301S human tau

These findings raised the question of whether a deficit in tau would also affect the dynactin complex. To this aim, we used mice transgenic for human tau with the FTDP-17 mutation P301S (Allen *et al*, 2002) and studied the distribution of tau and p150 in the axons of RGCs from organotypic cultures (Figure 7). We examined only axons with intact, continuous staining for neurofilament H, to avoid those with a general-

ized defect in axonal transport. RGCs prepared from these transgenic mice express human transgenic tau (Gasparini *et al*, 2006). Tau staining was strong and with some accumulations in RGC axons from transgenic mice (Figure 7A). This differed from what was observed in control mice, where tau staining was weaker and more homogeneously distributed (Figure 7B). In control RGCs, staining for p150 was concentrated in the distal axons and growth cones, as previously described (Abe *et al*, 1997), while it was weak in the proximal and intermediate portions of the axons. This stood in marked contrast to the irregular globular p150-immunoreactive structures, which colocalized with tau accumulation in axons from transgenic mice (Figure 7A). These findings are in agreement with an association between tau and p150, and suggest that tau dysfunction can result in the mislocalization of dynactin in axons even when neurofilament staining appears normal.

Discussion

An increasing number of studies supports the hypothesis that defects in axonal transport are responsible for neurodegenerative diseases (LaMonte *et al*, 2002; Holzbaur, 2004). Here we demonstrate a direct interaction between tau protein and dynactin p150, two MT-binding proteins, missense mutations in either of which can cause neurodegeneration (Puls *et al*, 2003, 2005; Yancopoulou and Spillantini, 2003; Münch *et al*, 2005).

Axonal MTs are organized with their fast-growing (plus) ends pointing towards the axonal tip. MTs are assembled in

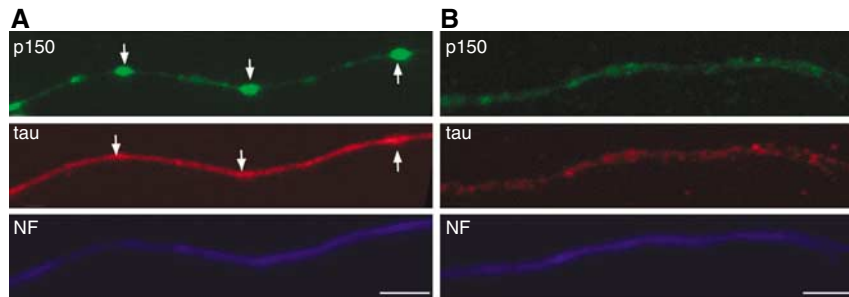


Figure 7 Colocalization of tau and p150 in RGC axons from P301S human tau transgenic mice. Retinal organotypic cultures from P301S human tau transgenic mice (A) and age-matched control mice (B) were cultured for 7 days and stained for p150 (green), tau (red) and neurofilament H (NF, blue). Arrows indicate the sites of accumulation of p150 and tau. Scale bars, 5 μ m. Axons shown here are representative of 150 fields observed in transgenic and control mice in three independent experiments.

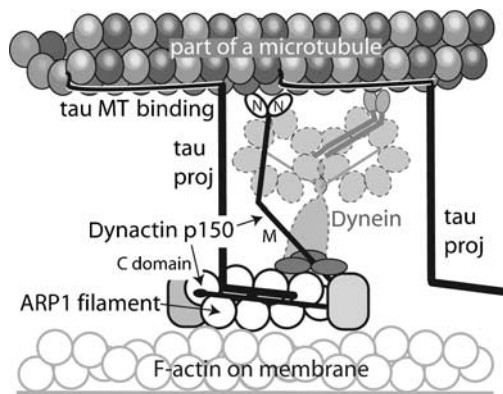


Figure 8 A model of the role of tau in stabilizing the interaction between axonal MTs and the dynein/dynactin complex. In this model the repeat region of tau binds to the inner surface of the MT lattice, part of tau (black line) binds to the outside surface, while the N-terminal domain projects away from the MT surface (Kar *et al*, 2003a, b). p150 binds to MT via its globular N-terminal domains. The interaction with tau might stabilize this association. Our data indicate that the projection domain of tau interacts with the C-terminal part of p150, which also binds to a short actin-like filament (Arp1 plus several other components; Imai *et al*, 2006). The latter part of the dynactin complex is able to contact vesicular cargoes as well as the cell membrane. Dynactin stabilizes the interaction of dynein with MT and mediates its binding to cargo.

the cell body and then transported along the axon (Baas *et al*, 2005). Tau is also found initially in the cell body, but after the development of one of the neurites into an axon, becomes concentrated in the distal axon. Kempf *et al* (1996) found that tau's localization to the distal axon requires intact MTs and microfilaments and proposed a model in which MT-bound tau is linked to the plasma membrane by a component that requires actin filaments for its subcellular localization. Our results suggest that the dynactin complex could be that component and support the idea that tau-stabilized MTs could be transported in the anterograde direction along the axon by dynein/dynactin motors linked to the axonal membrane. F-actin is another component of the anterograde axonal transport machinery and may be carried along with MTs through dynactin-mediated links as recently suggested (Fulga *et al*, 2007). Dynein/dynactin complexes also play a vital role in retrograde transport of vesicular cargoes. In this case, the presence of tau could help to assist dynein/dynactin interactions with MT tracks.

Our model of the molecular interaction between tau and p150 is shown in Figure 8. Both proteins bind independently to MTs. Tau can bind via multiple sites to several tubulin heterodimers, but may bind weakly to a small number of sites when excess amounts of tau are present. The binding site for p150 appears to overlap with some of the weaker binding sites for tau. However, when tau and p150 are present at physiological levels, they would be able to bind alongside each other, but to separate sites. According to our data, tau appears to stabilize the binding of the dynactin complex. The sequences of tau encoded by exons 1 and 4, which lie at the tip of the N-terminal projection domain, interact with the C-terminal region of p150. Neither exon 1 nor 4 appears to be essential for this interaction, with just one of them being sufficient; however, when exon 1 is present, an arginine at position 5 is required for p150 binding. A detailed structural study is needed to fully explain these complexities.

The C-terminal region of p150 to which the tau projection domain binds, occupies the portion of the dynactin complex that also projects away from MTs. Previously, the MT-binding proteins EB1 and CLIP170 have been shown to regulate the affinity of dynactin for MTs via the tubulin-binding N-terminal domain of p150 (Berrueta *et al*, 1999; Goodson *et al*, 2003; Lansbergen *et al*, 2004). Our findings suggest that tau facilitates the association of the dynactin complex with MT tracks by binding to the C-terminus of p150. Although other components of the dynactin complex bind to p150 in this extensive C-terminal region, a recent structural study has shown the presence of additional binding sites (Imai *et al*, 2006).

Our findings also indicate that the dysfunction of tau caused by FTDP-17 mutations, such as P301S, may affect the normal function of the dynactin complex. Further studies are needed to determine how a dysfunction in tau affects dynactin-related axonal transport. Our attempt to perform this study in RGC axons derived from P301S human tau transgenic mice (data not shown) has been hampered by a likely compensatory action of endogenous mouse tau on the effect of the human P301S mutant tau. Previous studies have shown that mouse tau is not involved in the aggregation of P301S tau (Allen *et al*, 2002). Missense *Tau* mutations reduce the ability of tau to interact with MTs, which may in turn result in the assembly of tau into abnormal filaments and impaired axonal transport (Hasegawa *et al*, 1998; Zhang *et al*, 2004). In RGC axons from mice transgenic for human P301S tau, p150 was redistributed and colocalized with abnormal

tau. Taken together, these results indicate that mutations in tau could lead to a redistribution of the dynactin complex and its reduced association with MTs, which could contribute to the clinical and neuropathological phenotype of FTDP-17 and other tauopathies.

Materials and methods

Antibodies

The following antibodies were used: polyclonal BR133 recognizing the N-terminus of tau and anti-p150(Glued) antibodies (BD Biosciences, San Jose, CA, USA) (Chemicon, Temecula, CA), anti-p150 antibody (DCTN1) (Abcam, Cambridge, UK) and SMI-31 monoclonal antibody (Sternberger Monoclonals Inc., Berkeley, CA) against phosphorylated neurofilament proteins.

Cloning, expression and purification of p150 and tau proteins

The coding sequences of the N-terminal part of tau isoforms were amplified from httau44, httau46 and httau40 cDNAs using the primers N-Tauf (5'-CTAGAATTCATGGCTGAGCCCC-3') and N-Taur (5'-CTACTCGAGAGCTGGGTACAGT-3'), and ligated into *EcoRI/XhoI*-cut pBT bait plasmid (Stratagene, La Jolla, CA). Full-length tau was amplified from httau40 cDNA using N-Tauf and Taur (5'-GACTCTCGAGTACAAAACCTG-3') primers and subcloned into pBT. p150 was cloned from human brain cDNA (Clontech, Mountain View, CA) using the primer pair p150f/p150r (5'-GACTCTCGAGTATGGCACAGAGCAAG-3'/5'-GACTGGTACCTTAGGAGATGAGCG-3') in a PCR reaction with Pfu Turbo polymerase (Stratagene, La Jolla, CA). The resulting PCR product was purified and ligated into *XhoI/KpnI*-cut pRSETB (Promega, Southampton, UK) for the expression of N-terminal His-tagged protein.

The coding sequences of tau fragments tau1-3, tau2-4 and tau5-13 (Figure 1) were amplified from httau40 cDNA using the primer pairs Tau1-3f/Tau1-3r (5'-CTAGAATTCATGGCTGAGCCCC-3'/5'-CTACTGAGTATGGTTCCTTC-3'), Tau2-4f/Tau2-4r (5'-CTAGAATTCGAACTCCCTGC-3'/5'-CTACTCGAGTATGGGTAC-3') and Tau5-13f/Tau5-13r (5'-CTAGAATTCGCTCGCATGGCT-3'/5'-CTACTCGAGTACAAAACCTG-3'), respectively, and subcloned into *EcoRI/XhoI*-digested pGEX-4T-1 (GE Healthcare, Piscataway, NJ). Fragments of human p150 were cloned into the vector pHis17 as described (Løwe and Amos, 1998) and the expressed His-tagged proteins p150N, p150M, p150C and full-length p150 were purified under native conditions by standard protocol on an Ni-NTA Superflow HPLC column, as instructed by the manufacturer (Qiagen, Hilden, Germany). Human tau fragments tau1-3, tau2-4 and tau5-13 (Figure 1) were cloned into pGEX-4T-1. GST-tagged tau fragments were expressed and purified on a GST affinity column under native conditions following the manufacturer's protocol (GE Healthcare, Piscataway, NJ). All affinity-purified p150.His and tau.GST protein fragments were run on a gel filtration Sephacryl S200 column (GE Healthcare, Piscataway, NJ) in buffer BRB80 (80 mM Pipes pH 6.8, 2 mM MgSO₄, 1 mM EGTA and 1 mM DTT) and concentrated before experiments; untagged wild-type and R5L- and R5H-mutant tau1-13 (htau40) were expressed and purified as described (Goedert and Jakes, 1990).

Bacterial two-hybrid screening

The screening was performed using BacterioMatch™ two-hybrid system (Stratagene, La Jolla, CA) in combination with a human brain plasmid cDNA library (Stratagene, La Jolla, CA). The cDNA library, cloned into BacterioMatch pTRG target vector, was amplified according to the manufacturer's instructions and purified using an EndoFree Plasmid Maxi kit (Qiagen, Hilden, Germany). BacterioMatch two-hybrid system reporter strain competent cells were cotransformed in pairwise combination of pTRG (containing the cDNA library) and pBT vector (containing the N-terminus of tau) and plated onto LB agar containing carbenicillin, tetracycline, chloramphenicol and kanamycin for selection of putative interacting clones. Colonies were amplified for further analysis and used as DNA template in PCR reactions with pTRGf (5'-CAGCCTGAAGT GAAAGAA-3') and pTRGr (5'-ATTCGTCGCCGCCATAA-3') primers. DNA was purified using the PCR product purification kit (Roche Diagnostics, Basel, Switzerland), sequenced and analyzed using BLAST against the NCBI nucleotide database.

Purification of tubulin and dynactin complex from pig brains

Tubulin was purified from pig brain as described (Hyman *et al*, 1991). Pig brain dynactin complex was prepared using a published protocol (Bingham *et al*, 1998) and checked by immunoblotting (Supplementary Figure). SDS-PAGE of the purified fraction showed the numerous components of the complex, including p150, p50, ARP1, p25 and p20. However, it did not include any of the p135 isoform lacking the N-terminal globular domain.

In vitro binding and immunoprecipitation

GST-tagged tau and His-tagged p150 fragments and full-length recombinant or native proteins were used for *in vitro* binding. GST- and His-tagged proteins were immobilized onto magnetic beads coated with anti-GST or anti-His antibodies. Anti-His and anti-GST antibody magnetic beads, MACS[®] MicroBeads (Miltenyi Biotec GmbH, Bergisch Gladbach, Germany), were used for studying the interactions of tau, p150 and their fragments. Antibody-targeted protein was first incubated with the appropriate antibody coupled to magnetic beads in buffer BRB80 at 30°C for 20 min. An aliquot of magnetically labelled protein was then incubated with each candidate interacting protein for a further 20 min. The protein complexes were eluted from the beads using a MACS μ Column according to the manufacturer's instructions and analyzed by SDS-PAGE stained by PAGE BLUE 83.

MT pelleting assay

In vitro binding of pig brain dynactin complex to MTs polymerized from pig brain tubulin with and without recombinant tau was assayed by co-sedimentation. Only full-length tau (wild-type or N-terminally mutated) was used in these experiments, since tau5-13 was very poor in promoting MT assembly. Binding of proteins to MTs was assayed by *in vitro* co-sedimentation analysis. Tubulin (10 μ M) was assembled with or without 4 μ M tau for 30 min at 35°C in BRB80 buffer containing 2 mM of the non-hydrolysable GTP analogue GMP.CPP. Pig brain dynactin complex (5 μ M) was then incubated with MTs for a further 20 min at 30°C, before a 20-min centrifugation at 96 600 g. Supernatants and pellets were analyzed using 12.5% SDS-PAGE.

Electron microscopy

MTs were polymerized from pig brain tubulin in BRB80 buffer with or without full-length tau protein, as described for the pelleting assay, and then incubated with pig brain dynactin complex at 30°C for a further 20 min. The specimens were negatively stained with 2% uranyl acetate and observed using a Philips EM208 TEM. Images were taken at 50K magnification.

For immunoelectron microscopy, specimens were prepared as described by Melkonian *et al* (2007), using an anti-p150 antibody (DCTN1) followed by protein A conjugated to 20 nm gold (BB International, Cardiff, UK). Cytochrome c (1%) was included in each solution as blocking agent. Grids were stained with 0.5–1% uranyl acetate and observed using a Philips EM208S TEM with a magnification of 28K, and micrographs were recorded using a Gatan ES1000W CCD Camera

Cultures and immunocytochemistry of SH-SY5Y cells

The SH-SY5Y human neuroblastoma cell line was grown in Dulbecco's modified Eagle medium (DMEM; Invitrogen, Paisley, UK) supplemented with penicillin (20 U/ml), streptomycin (20 mg/ml) and 15% v/v heat-inactivated fetal calf serum (Invitrogen, Paisley, UK). Cells were maintained at 37°C in 5% CO₂ and seeded at a density of 10⁴ cells/cm² on Petri dishes or coverslips. Differentiation was carried out by treatment with 10 μ M RA (Sigma, Poole, UK) for 2 weeks and with 50 ng/ml BDNF (R&D Systems, Minneapolis, MN) for 4 days. Differentiated SH-SY5Y cells were fixed with 4% paraformaldehyde in PBS and incubated overnight with the primary antibody (anti-tau BR133; anti-p150, BD Biosciences, San Jose, CA) diluted in 5% serum, 0.25% Triton X-100 in PBS. Following incubation with Alexa 488- and 568-conjugated secondary antibodies (Molecular Probes, Invitrogen, Paisley, UK), coverslips were mounted using the ProLong anti-fade kit (Molecular Probes, Invitrogen, Paisley, UK).

Preparation of cell extracts and immunoblotting

Differentiated SH-SY5Y cells were harvested in lysis buffer (25 mM Tris-HCl pH 7.4, 150 mM NaCl, 0.1% v/v Nonidet P-40 and complete protease inhibitor cocktail; Roche Diagnostics, Basel,

Switzerland) and disrupted on ice by repeated passage through a 25-gauge syringe needle. Lysates were precleared with protein A/G-Sepharose suspension (50–100 µl/ml) and incubated overnight at 4°C with specific antibodies. Immunoglobulins from the same species as the primary antibody were used as controls. Immuno-complexes were then adsorbed with protein A-Sepharose beads. The supernatants were collected and the beads thoroughly washed and resuspended in 50 mM Tris-HCl, pH 7.4. Supernatants and pellets were analyzed by SDS-PAGE followed by immunoblotting.

Proteins (20–30 µg) from lysates or immunoprecipitates were separated on 9–15% SDS-PAGE gels and transferred onto Immobilon-P nitrocellulose membranes (Millipore, Bedford, MA). Membranes were incubated for 1 h with 4% w/v Marvel milk (Premier International Foods, Spalding, UK) in TBS and probed with primary antibody (anti-p150, Chemicon, Temecula, CA), followed by peroxidase-conjugated secondary antisera (1:2000). After washing, the blots were developed using enhanced chemiluminescence (Amersham Biosciences, Bucks, UK).

Organotypic culture of retinal ganglion neurons

Organotypic cultures of RGCs were established from C57/BL6 mice and homozygous P301S tau transgenic mice at 5 months of age, as described (Bates and Meyer, 1993). Briefly, the mice were anesthetized with CO₂ and killed by cervical dislocation. The eyes were removed and immediately placed in sterile Hank's Balanced Salt Solution (HBSS) supplemented with 5 mM Hepes, 44 mM sodium bicarbonate and 16 mM glucose. The retina was removed under sterile conditions and sectioned into 400-µm squares using a McIlwain tissue chopper. The retinal segments were then placed on acid-cleaned glass coverslips coated with 0.5 mg/ml poly-D-lysine for 4–6 h, followed by 5 µg/ml EHS laminin for overnight. The explants were kept in DMEM serum-free media containing 25 mM Hepes pH 7.4, 2 mM L-glutamine, 5 µg/ml bovine insulin, 100 µg/ml apotransferrin, 20 nM progesterone, 100 nM putrescine, 30 nM

selenium, 100 µM pyruvate 76 µg/ml BSA and 50 µg/ml gentamicin (All from Invitrogen, Paisley, UK) and maintained at 37°C, 5% CO₂. Consistent with previous findings (Bates and Meyer, 1997), 74 ± 5% (percentage ± s.e.m.) of retinal explants showed axonal outgrowth. No significant difference in axonal outgrowth efficiency was detected between the cultures from human P301S tau transgenic and C57/BL6 control mice (Gasparini *et al*, 2006). Immunohistochemical analysis of tau and p150 was performed on retinal cultures at 7 days *in vitro*. Cultures were fixed with cold methanol for 5 min, blocked with 2% goat serum, 1% bovine serum albumin (BSA), 0.1% gelatin in TBS containing 0.1% Triton-X100 and incubated overnight at 4°C with primary antibodies diluted in 1% BSA, 0.1% gelatin in PBS. For the anti-p150 antibody, the Alexa 488-tyramide amplification system was used (Invitrogen, Paisley, UK). For anti-tau and anti-neurofilament antibodies, Alexa 568-conjugated anti-rabbit and Alexa-350-conjugated anti-mouse secondary antibodies were used. Coverslips were mounted using Permafluor (Lipshaw, Pittsburgh, PA) mounting medium. Each reported immunohistochemical staining was performed at least three times and four coverslips were used for each staining.

Supplementary data

Supplementary data are available at *The EMBO Journal* Online (<http://www.embojournal.org>).

Acknowledgements

We thank Drs R Meyer and J Miotke for help in setting up the retinal cultures. EM and LG are the recipients of an Alzheimer's Research Trust studentship and fellowship, respectively. This work was supported by the UK Alzheimer's Research Trust, the Medical Research Council and Cancer Research UK.

References

- Abe TK, Tanaka H, Iwanaga T, Odani S, Kuwano R (1997) The presence of the 50-kDa subunit of dynactin complex in the nerve growth cone. *Biochem Biophys Res Commun* **233**: 295–299
- Allen B, Ingram E, Takao M, Smith MJ, Jakes R, Virdee K, Yoshida H, Holzer M, Craxton M, Emson PC, Atzori C, Migheli A, Crowther RA, Ghetti B, Spillantini MG, Goedert M (2002) Abundant tau filaments and non-apoptotic neurodegeneration in transgenic mice expressing human P301S tau protein. *J Neurosci* **22**: 9340–9351
- Baas PW, Karabay A, Qiang L (2005) Microtubules cut and run. *Trends Cell Biol* **15**: 518–524
- Bates CA, Meyer RL (1993) The heavy neurofilament protein is expressed in regenerating adult but not embryonic mammalian optic fibers *in vitro*. *Exp Neurol* **119**: 249–257
- Bates CA, Meyer RL (1997) The neurite-promoting effect of laminin is mediated by different mechanisms in embryonic and adult regenerating mouse optic axons *in vitro*. *Dev Biol* **181**: 91–101
- Berrueta L, Tirnauer JS, Schuyler SC, Pellman D, Bierer BE (1999) The APC-associated protein EB1 associates with components of the dynactin complex and cytoplasmic dynein intermediate chain. *Curr Biol* **9**: 425–428
- Bingham JB, King SJ, Schroer TA (1998) Purification of dynactin and dynein from brain tissue. *Methods Enzymol* **298**: 171–184
- Brandt R, Leger J, Lee G (1995) Interaction of tau with the neural plasma membrane mediated by tau's amino-terminal projection domain. *J Cell Biol* **131**: 1327–1340
- Chen J, Kanai Y, Cowan NJ, Hirokawa N (1992) Projection domains of MAP2 and tau determine spacings between microtubules in dendrites and axons. *Nature* **360**: 674–677
- Fulga TA, Elson-Schwab I, Khurana V, Steinhilb ML, Spires TL, Hyman BT, Feany MB (2007) Abnormal bundling and accumulation of F-actin mediates tau-induced neuronal degeneration *in vivo*. *Nat Cell Biol* **9**: 139–148
- Gasparini L, Goedert M, Spillantini MG (2006) Hyperphosphorylated tau accumulates in retinal ganglion neurons of P301S tau transgenic mice. *Alzheimers Dement* **3** (Suppl 1): S120
- Goedert M, Jakes R (1990) Expression of separate isoforms of human tau protein: correlation with the tau pattern in brain and effects on tubulin polymerization. *EMBO J* **9**: 4225–4230
- Goedert M, Spillantini MG, Jakes R, Rutherford D, Crowther RA (1989) Multiple isoforms of human microtubule-associated protein tau sequences and localization in neurofibrillary tangles of Alzheimer's disease. *Neuron* **3**: 519–526
- Goodson HV, Skube SB, Stalder R, Valetti C, Kreis TE, Morrison EE, Schroer TA (2003) CLIP-170 interacts with dynactin complex and the APC-binding protein EB1 by different mechanisms. *Cell Motil Cytoskeleton* **55**: 156–173
- Hasegawa M, Smith MJ, Goedert M (1998) Tau proteins with FTDP-17 mutations have a reduced ability to promote microtubule assembly. *FEBS Lett* **437**: 207–210
- Hayashi S, Toyoshima Y, Hasegawa M, Umeda Y, Wakabayashi K, Tokiguchi S, Iwatsubo T, Takahashi H (2002) Late-onset frontotemporal dementia with a novel exon 1 (Arg5His) tau gene mutation. *Ann Neurol* **5**: 525–530
- Hirokawa N, Shiomura Y, Ogabe S (1988) Tau proteins: the molecular structure and mode of binding on microtubules. *J Cell Biol* **107**: 1449–1459
- Holzbaier EL, Hammarback JA, Paschal BM, Kravit NG, Pfister KK, Vallee RB (1991) Homology of a 150K cytoplasmic dynein-associated polypeptide with the *Drosophila* gene Glued. *Nature* **351**: 579–583
- Holzbaier EL (2004) Motor neurons rely on motor proteins. *Trends Cell Biol* **14**: 233–240
- Hyman A, Drechsel D, Kellogg D, Salser S, Sawin K, Steffen P, Wordeman L, Mitchison T (1991) Preparation of modified tubulins. *Methods Enzymol* **196**: 478–485
- Imai H, Narita A, Schroer TA, Mada Y (2006) Two-dimensional averaged images of the dynactin complex revealed by single particle analysis. *J Mol Biol* **359**: 833–839
- Kempf M, Clement A, Faissner A, Lee G, Brandt R (1996) Tau binds to the distal axon early in development of polarity in a microtubule- and microfilament-dependent manner. *J Neurosci* **16**: 5583–5592

- Kar S, Fan J, Smith MJ, Goedert M, Amos LA (2003a) Repeat motifs of tau bind to the insides of microtubules in the absence of taxol. *EMBO J* **22**: 70–77
- Kar S, Florence GJ, Paterson I, Amos LA (2003b) Discodermolide interferes with the binding of tau protein to microtubules. *FEBS Lett* **539**: 34–36
- LaMonte BH, Wallace KE, Holloway BA, Shelly SS, Ascano J, Tokito M, van Winkle T, Howland DS, Holzbaur EL (2002) Disruption of dynein/dynactin inhibits axonal transport in motor neurons causing late-onset progressive degeneration. *Neuron* **34**: 715–727
- Lansbergen G, Komarova Y, Modesti M, Wyman C, Hogenraad CC, Goodson HV, Lemaitre RP, Drechsel DN, van Munster E, Gadella Jr TW, Grosveld F, Galiart N, Borisy GG, Akhmanova A (2004) Conformational changes in CLIP-170 regulate its binding to microtubules and dynactin localization. *J Cell Biol* **166**: 1003–1014
- Lee VM-Y, Goedert M, Trojanowski JQ (2001) Neurodegenerative tauopathies. *Annu Rev Neurosci* **24**: 1121–1159
- Løwe J, Amos LA (1998) Crystal structure of the bacterial cell-division protein FtsZ. *Nature* **391**: 203–206
- Makrides V, Massie MR, Feinstein SC, Lew J (2004) Evidence for two distinct binding sites for tau on microtubules. *Proc Natl Acad Sci USA* **101**: 6746–6751
- Melkonian KA, Maier KC, Godfrey JE, Rodgers M, Schroer TA (2007) Mechanism of dynamitin-mediated disruption of dynactin. *J Biol Chem* **282**: 19355–19364
- Münch C, Rosenbohm A, Sperfeld AD, Uttner I, Reske S, Krause BJ, Sedlmeier R, Meyer T, Hanemann CO, Stumm G, Ludolph AG (2005) Heterozygous R1101K mutation of the DCTN1 gene in a family with ALS and FTD. *Ann Neurol* **58**: 777–780
- Poorkaj P, Muma NA, Zhukareva V, Cochran EJ, Shannon KM, Hurtig H, Koller WC, Bird TD, Trojanowski JQ, Lee VM-Y, Schellenberg GD (2002) An R5L tau mutation in a subject with a progressive supranuclear palsy phenotype. *Ann Neurol* **52**: 511–516
- Puls I, Jonnakuty C, LaMonte BH, Holzbaur EL, Tokito M, Mann E, Floeter MK, Bidus K, Drayna D, Oh SJ, Brown RH, Ludlow CL, Fischbeck KH (2003) Mutant dynactin in motor neuron disease. *Nat Genet* **33**: 455–456
- Puls I, Oh SH, Sumner CJ, Wallace KE, Floeter MK, Mann EA, Kennedy WR, Wendelschafer-Crabb G, Vortmeyer A, Powers R, Finnegan K, Holzbaur EL, Fischbeck KH, Ludlow CL (2005) Distal spinal and bulbar muscular atrophy caused by dynactin mutation. *Ann Neurol* **57**: 687–694
- Schafer DA, Gill SR, Cooper JA, Heuser JE, Schroer TA (1994) Ultrastructural analysis of the dynactin complex: an actin-related protein is a component of a filament that resembles F-actin. *J Cell Biol* **126**: 403–412
- Schroer TA (2004) Dynactin. *Annu Rev Cell Dev Biol* **20**: 759–779
- Waterman-Storer CM, Karki S, Holzbaur EL (1997) The interaction between cytoplasmic dynein and dynactin is required for fast axonal transport. *Proc Natl Acad Sci USA* **94**: 12180–12185
- Waterman-Storer CM, Karki S, Holzbaur EL (1995) The p150Glued component of the dynactin complex binds to both microtubules and the actin-related protein centractin (Arp-1). *Proc Natl Acad Sci USA* **92**: 1634–1638
- Yancopoulou D, Spillantini MG (2003) Tau protein in familial and sporadic diseases. *Neuromol Med* **4**: 37–48
- Zhang B, Higuchi M, Yoshiyama Y, Ishihara T, Forman MS, Martinez D, Joyce S, Trojanowski JQ, Lee VM-Y (2004) Retarded axonal transport of R406W mutant tau in transgenic mice with a neurodegenerative tauopathy. *J Neurosci* **24**: 4657–4667